P3.24   **A REVISED APPROACH TO SUBGRID-SCALE CLOUD PROCESSES
IN A CUMULUS PARAMETERIZATION SCHEME AND ITS EFFECTS ON SEASONAL PREDICTION**

Young-Hwa Byun*, Song-You Hong,
Department of Atmospheric Sciences, Global Environmental Laboratory, Yonsei University, Seoul, Korea

Won-Tae Yun
Climate Prediction Division, Korea Meteorological Administration, Seoul, Korea

1. INTRODUCTION

Moist convection plays a central role in most of the interactions to the physical processes such like dynamical, hydrodynamical, radiative and surface processes. Therefore, the parameterization of the moist convection has been treated as one of the most important tasks, particularly, in general circulation model (GCM) with coarse resolutions. While many works have been performed in order to further develop and improve cumulus parameterization scheme, previous studies have pointed out that the representation of the subgrid-scale convective processes in the mass-flux convective parameterization scheme influence the model climate considerably in GCMs (e.g., Cheng and Arakawa 1991, Hong 2000, Donner et al. 2001, Lin and Neelin 2001). For example, Lin and Neelin (2001) showed that subgrid-scale variability in the moist convection scheme strongly interacts with large-scale dynamics, and the response of the large-scale to smaller-scale variability might be a substantial percentage of the large-scale variance observed in precipitation.

The simplified Arakawa-Schubert (SAS) scheme of Pan and Wu (1995) has been operational at the National Centers for Environmental Prediction (NCEP) Medium-Range Forecast (MRF) model since 1993. Subsequent development of the SAS scheme has been made to improve the predictability of weather forecasts (Hong and Pan 1996, 1998, Hong 2000). More recently, important modifications were introduced to the subgrid-scale convective properties of the cloud model within the scheme as follows;

Corresponding author : Song-You Hong, Department of Atmospheric Sciences, Yonsei University, Seoul 120-749, Korea. E-mail: shong@yonsei.ac.kr

Current affiliation: Young-Hwa Byun, Climate Prediction Division, Korea Meteorological Administration. E-mail: yhbyun@kma.go.kr

consideration of stochastic cloud processes (multiple clouds), parameterization of convective momentum transport.

Another important modification to the SAS scheme, which is an inclusion of explicit large-scale destabilization effect considering synoptic scale moisture convergence, will be introduced in this study. Each component of revisions will be evaluated for simulated tropical precipitation in response to SST anomalies.

2. PARAMETERIZATION OF SUBGRID-SCALE CONVECTIVE PROCESSES

The NCEP MRF model is a global spectral model (Sela 1980). Subsequent developments were described in Kanamitsu (1989), Kanamitsu et al. (1991), Hong and Pan (1996), Caplan et al. (1997) and Kanamitsu et al. (2002a). The NCEP MRF model utilized in this study is a version of the model with the physics package that was operational as of January 2000.

a. Parameterization of stochastic cloud processes and convective momentum transport

In the current SAS scheme, the cloud top level is determined as a highest top level where the buoyancy force of the parcel becomes zero, while the detrainment originating level by downdraft is fixed as a level where environmental moist static energy is a minimum. In the modified scheme, the actual cloud top level is determined randomly between the highest top level and the detrainment originating level. Once the actual cloud top level is determined, the proper entrainment rate is re-calculated in order that the air parcel becomes neutral at the actual cloud top. For the treatment of convective momentum transport, we follow the parameterization method implemented at the NCEP (Global Climate and Weather Modeling Branch, 2003). This method is based on the work of Wu and Yannai (1994). The convective momentum parameterization consists of the formulations for the

subsidence of environmental air that compensates the cloud mass flux, the detrainment of momentum from clouds, and the convective-scale horizontal pressure gradient force.

b. Large-scale destabilization effect

The quasi-equilibrium assumption is represented as follows.

$$\left[\frac{dA}{dt}\right]_{LS} + \left[\frac{dA}{dt}\right]_{CU} \approx 0 , \qquad (1)$$

where the subscript LS and CU denote the large-scale and cumulus contribution, respectively. The destabilization of an air parcel by the large-scale atmosphere is nearly balanced by the stabilization of the cumulus. The CWF A' calculated from the environment and the climate CWF A^0 derived from the observations by Lord et al. (1982) provide an estimate of the large-scale destabilization by the following:

$$\left[\frac{dA}{dt}\right]_{LS} = \frac{A' - f(x)A_0}{\Delta t} . \qquad (2)$$

In Eq. (2), we assume that the climate CWF is modified by the large-scale contribution $f(x)$. This implies that the large-scale destabilization should be specified as the rate at which the given instability of an air column will be neutralized and should be different based on the large-scale forcing of the environment, as discussed in Pan and Wu (1995). Thus, the function $f(x)$ is defined as

$$f(x) = \frac{1}{\pi}\left[\frac{\pi}{2} - Tan^{-1}(\frac{x}{a} - b)\right], \qquad (3)$$

$$x = \int_{p_{sfc}}^{p_{cloud\_top}} \left\langle -\vec{\nabla} \cdot q\vec{V} \right\rangle_p dp / \Delta p . \qquad (4)$$

Here, x represents the large-scale moisture convergence, which is spatially averaged over the certain effective space. The bracket in Eq. (4) means the horizontally weighted value at the pressure level. Vertical integration of the large-scale moisture convergence is operated from the surface to the cloud top level, and this is normalized by the pressure difference $\Delta p = p_{cloud\_top} - p_{sfc}$. In Eq. (3), a constant a denotes the reference value to normalize x. This constant is determined as a maximum limit of the large-scale moisture convergence obtained from the monthly mean of NCEP reanalysis II data (Kanamitsu et al. 2002) during 25 years from 1979 to 2003. This a sets as 4×10^{-8} sec^{-1}. Meanwhile, a constant b is fixed as 3.0 to determine the proper

estimate of the large-scale destabilization. The adjustment time scale Δt sets to 30 min in this study.

3. THE MODEL AND EXPERIMENTAL SETUP

To investigate the effect of the revised parameterization on the seasonal prediction, we performed five experiments in Table 1. The MRF model utilized in this study employs a resolution of T62L28. To avoid introducing uncertainties with the initial data, 5-member ensemble runs for each experiment were performed with an approximate 4-week lead time for the boreal summer (June-July-August) of 1996, 1997, and 1999. The initial data for each ensemble was taken from the NCEP reanalysis II data (Kanamitsu et al. 2002b), starting from 0000 UTC 1 May to 0000 UTC 5 May with a 24-hr interval. As a surface boundary condition, observed sea surface temperature (SST) data were used with a resolution of 1° (Raynolds and Smith 1994) during the simulation period. For evaluations, observed precipitation was taken from the Climate Prediction Center (CPC) Merged Analysis Monthly Precipitation data (CMAP) (Xie and Arkin 1997), and observed large-scale fields were taken from the NCEP reanalysis II data (Kanamitsu et al. 2002b).

Table 1. Summary of numerical experiments.

Expr.	Description
CNTL	Control run
STCP	CNTL with the stochastic cloud processes
CMTP	CNTL with the convective momentum transport
LSDP	CNTL with the large-scale destabilization effect
SALL	CNTL with all processes mentioned above

4. THE IMPACT ON THE MODEL CLIMATE

a. Precipitation

Table 2 shows the impact of the revised parameterization method on the global precipitation pattern for each year. Overall, the revised parameterization scheme (SALL) improves the global precipitation distribution. Compared with the observation, the CNTL run shows approximately 30% more precipitation amount and pattern correlation coefficient of 0.64~0.67 through three years. The

SALL experiment decreases the global rainfall amount to approximately 10% as compared to the CNTL case, but its precipitation pattern is improved, showing the correlation coefficient of 0.71~0.76. In this table, it is obvious that each component operates to decrease the excessive rainfall amount as shown in the CNTL run. However, it is also clear that the STCP and LSDP cases keep the precipitation pattern similar to the observation, but the CMTP case does not.

Table 2. Global mean precipitation (mm day^{-1}) and the pattern correlation coefficient (parentheses) between the CMAP data and simulated results for the global precipitation.

| | Year | | |
	1996	1997	1999
CMAP	2.71	2.73	2.55
CNTL	3.55 (0.67)	3.62 (0.64)	3.57 (0.66)
STCP	3.46 (0.75)	3.49 (0.70)	3.48 (0.52)
CMTP	3.41 (0.64)	3.45 (0.57)	3.45 (0.48)
LSDP	3.50 (0.70)	3.58 (0.65)	3.52 (0.69)
SALL	3.35 (0.76)	3.38 (0.73)	3.36 (0.71)

To examine the difference of precipitation pattern due to each modification, summer mean precipitations averaged for 3 years (1996, 1997, and 1999) are represented in Fig. 1. (All figures in this section show three-year means.) The CNTL case reproduces the tropical rainfall fairly well. However, it is apparent that the CNTL experiment has some discernible defects: the excessive rainfall in the trade wind region north of the equator and underestimated precipitation over the equatorial western Pacific near the Maritime Continent.

Other experiments show good agreement with the observation for the global precipitation, but they have distinct features for each modification. First, the STCP case reproduces the rainfall pattern similar to the observation. It is due to the reduction of the excessive rainfall along the trade wind region north of equator and more organized rainfall over the western ITCZ. In the CMTP case, overall decrease of the rainfall occurs over the western Pacific, but not over the eastern Pacific. Too much decrease of the rainfall over the western Pacific in the CMTP case leads to worse pattern, when compared with the observation. The LSDP run produces similar pattern to the CNTL case over the whole Pacific area. In the SALL experiment including all modifications, precipitation pattern

becomes closer to the observation, although the rainfall over the eastern Pacific tends to increase. Such an improvement in the SALL experiment is due to the decrease of excessive rainfall in the north-western Pacific area near 20°N and representation of SPCZ close to the observation. Consequently, the SALL experiment leads to the well-organized convection system over the western Pacific as a combined effect of three modifications, so that it shows a considerable improvement on simulation of the precipitation.
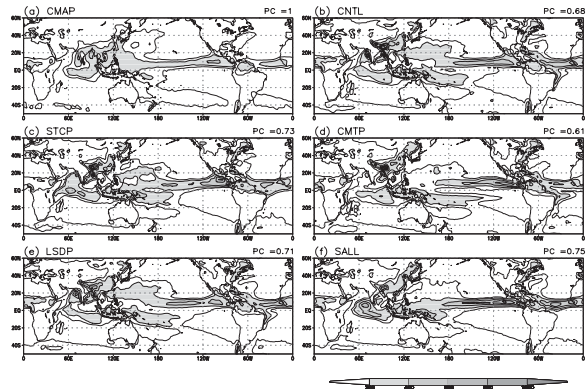
Fig. 1. Mean precipitation (mm month^{-1}) averaged for the summers of the 3 years (1996, 1997, and 1999) for (a) the observation and (b),(c),(d),(e),(f) each experiments. Contour intervals are 200 mm, except for that the first contour designates 100 mm. Shading designates the precipitation amount greater than 200 mm. The values marked in the upper-right of each panel indicate pattern correlation coefficients between the observation and simulated results over the plotting area.

b. Role of modified processes in the large-scale adjustment

In Fig. 2., it is apparent that temperature and moisture of the STCP experiment becomes colder and wetter in the upper troposphere and in the lower troposphere below 600~700 hPa level. In the middle layer, the STCP case produces warmer and drier atmosphere. The SAS scheme allows the only deepest cloud top. As well, detrainment of the SAS scheme occurs only at the cloud top level. Therefore, selection of the lower cloud tops in the STCP case results in more detrainment in the upper troposphere below the highest cloud top level where the cloud top of the CNTL case is located. This directly leads to the increase of moisture in the upper troposphere, and then leads to the decrease of temperature. On the

other hand, large differences in temperature field occur in the middle troposphere due to the stochastic cloud processes. This feature is probably related to the radiative warming due to the lower level clouds than those of the CNTL case.
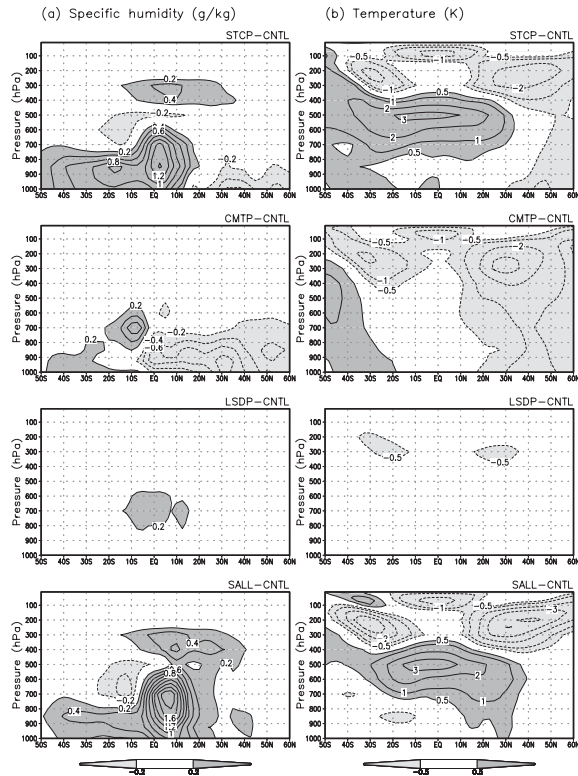
Fig. 2. Zonal mean differences between the CNTL experiment and other experiments for (a) the specific humidity (g kg^{-1}) and (b) the temperature (K). Dark shading designates the values greater than +0.2 g kg^{-1}/+0.5 K, and light shading designates the values smaller than –0.2 g kg^{-1}/-0.5 K.

In the CMTP case, maxima of the temperature difference occur in the upper troposphere, similar to the STCP case. However, temperature difference as same as the STCP case does not occur in the middle layer. For the moisture difference, low-level moisture decreases overall in the northern hemisphere, whereas the slight increase of the moisture appears near 10°S. The CMTP case decelerates the zonal and the meridional winds in the tropical upper troposphere, and thus it affects on the large-scale circulation. In particular, the CMTP case shows weakening and southward moving of the Hadley circulation (see Fig. 3). Therefore, weakening of the meridional circulation directly produces less transport of the low-level moisture, and then leads to the decrease of the low-level moisture over the ITCZ in the CMTP run. Concerning with the heat transport, large temperature difference appears in the upper troposphere. This feature is probably due to the less transport toward mid-latitude of both hemisphere and also is presumably due to decrease of the adiabatic warming in the sinking branches of the meridional circulation.

Meanwhile, impact of the LSDP on the large-scale field as well as precipitation is not obvious. Finally, it is clear that the SALL case shows very similar differences in temperature and moisture fields to the STCP case. This means that the selection process of the cloud top is the most sensitive factor among the modifications in this study on simulation of the model climate. However, it is also obvious that other modifications are non-linearly combined into to the SALL case, and consequently this revised SAS scheme leads to the improvement of the precipitation pattern due to the intensifying of the western Pacific ITCZ.
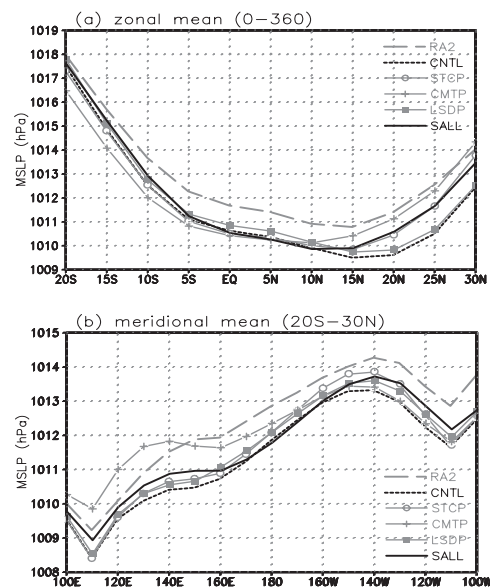
Fig. 3. Mean sea level pressure (hPa) for the observation (RA2) and each experiment. (a) represents the zonal mean (0° ~ 360°) pressure, and (b) indicates the meridional mean (20°S ~ 30°N) pressure.

c. Large-scale circulation

The change in the Walker circulation and/or the Hadley circulation is clearly detected by the change in sea level pressure (Fig. 3). When compared with the

observation, all experiments have negative biases on the sea level pressure in general. In Fig. 3, it is easily seen that the SALL experiment tends to improve this error. The meridional circulation of the SALL experiment is improved considerably in the rising branch of the Hadley cell, compared with the CNTL case. One noticeable feature in Fig. 3(a) is southward movement of the Hadley cell due to the CMTP case.

In this study, inclusion of the convective momentum transport results in the slight movement of the meridional circulation as well as its weakening. Meanwhile, change in the zonal flow for each experiment is not large, except for the CMTP case (Fig. 3b). The CMTP case shows the higher pressure over the western Pacific than those of other experiments. This means less convection over the western Pacific due to weakening of the low-level moisture convergence.

d. Effect of the non-linear interaction

In the previous sub-section, it is clear that the STCP and the CMTP experiments have a considerable influence on the model climate. However, the LSDP experiment does not seem to play an important role in improving the global precipitation and associated large-scale circulation. The additional experiment was performed to investigate a role of the large-scale destabilization processes in the revised SAS scheme, and effect of non-linear interaction between the LSDP and other processes will be described in this sub-section. The additional experiment is entitled "NLSD", and consists of 5-member ensemble runs with the STCP and the CMTP processes excluding the LSDP case for 3-year summers.

For the precipitation difference (Fig. 4), it is obvious that the NLSD experiment decreases tropical precipitation along the ITCZ, as compared to the SALL experiment. In particular, it is easily shown that dry tongue penetrates through the Indonesian area over the western Pacific, so that the rainfall is reduced considerably, as compared to the observation. On the other hand, precipitation of the NLSD case tends o be increased in the SPCZ. Consequently, such a change compared to the SALL case leads to the lower pattern correlation coefficient, because equatorial rainfall over the western Pacific is reduced too much in the NLSD experiment.

This pattern of the NLSD case is related to the position of Hadley circulation. In the sea level pressure pattern, the NLSD experiment shows higher pressure over the eastern and the central Pacific

areas than that of the SALL cases (figure is not shown). This can leads to the enhanced tropical Walker circulation. However, the Hadley circulation is clearly moved toward the south in the NLSD case, though its strength does not seem to be changed. Accordingly, we can say that the large-scale destabilization processes have an important role in controlling the large-scale circulation together with the STCP and CMTP cases through non-linear interaction, although its single effect is not large on the model climate.
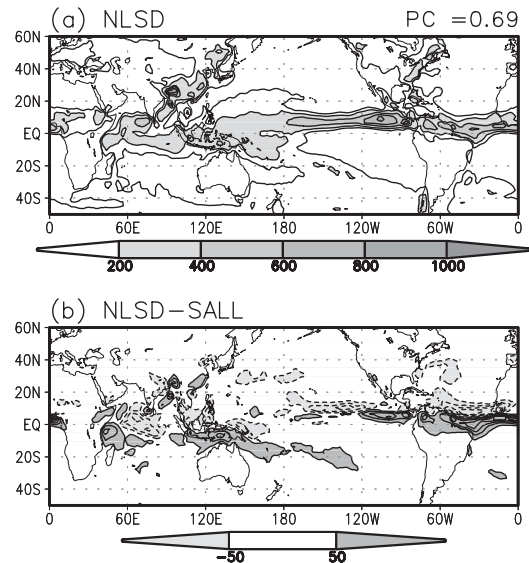
Fig. 4. Same as Fig. 1, but except for the NLSD case and the difference from the SALL experiment.

5. CONCLUSION

In this study, the recently-developed subgrid-scale convective properties in the SAS scheme in the NCEP MRF model has been evaluated for the simulation of tropical rainfall. The revised parameterization method (that is, the SALL experiment) improves the precipitation fields due to the better representation of the well-organized convective system over the western Pacific. This improvement results from the combined effect of three modifications for the convective processes, accompanying with the change in the large-scale circulation – intensification of the Hadley circulation.

According to the result of Jung and Arakawa (2004), model physics, in particular, associated with the cloud processes is highly dependent on the model resolution. Because this study is limited in the result of the model with low resolution, investigating the

impact of the revised parameterization method in a model with high resolution requires further study.

REFERENCES

Caplan, P., J. Derber, W. Gemmill, S.-Y. Hong, H.-L. Pan, and D. Parrish, 1997: Changes to the 1995 NCEP operational medium-range forecast model analysis-forecast system. *Wea. and Forecasting*, 12, 581-594.

Cheng, M.-D., and A. Arakawa, 1991: Inclusion of convective downdrafts in the Arakawa-Schubert cumulus parameterization. *19th Conf. On Hurricane and Tropical Meteorology*. Miami, FL, Amer. Meteor. Soc., 295-300.

Donner, L. J., C. J. Seman, and R. S. Hemler, 2001: A cumulus parameterization including mass fluxes, convective vertical velocities, and mesoscale effects: Thermodynamic and hydrological aspects in a general circulation model. *J. Climate*, **14**, 3444-3463.

Global Climate and Weather Modeling Branch, 2003: The GFS atmospheric model. NCEP office note 442, 14 pp. [Available online at http://wwwt.emc.ncep.noaa.gov/officenotes.]

Hong, S.-Y., 2000: Impact of the subgrid representation of parameterized convection on simulated climatology. NCEP office note 428, 32 pp. [Available from NCEP/EMC, 5200 Auth Road, Camp Springs MD 20746.]

_____, and H.-L. Pan, 1996: Nonlocal boundary layer vertical diffusion in a Medium-Range Forecast model. *Mon. Wea. Rev.,* **124**, 2322-2339.

_____, and _____, 1998: Convective trigger function for a mass flux cumulus parameterization scheme. *Mon. Wea. Rev.*, **126**, 2599-2620.

Jung, J.-H., and A. Arakawa, 2004: The resolution dependence of model physics: Illustrations from nonhydrostatic model experiments. *J. Atmos. Sci.*, **61**, 88-102.

Kanamitsu, M., 1989: Description of the NMC global data assimilation and forecast system. *Wea. and Forecasting*, **4**, 335-342.

_____, and Coauthors, 1991: Recent changes implemented into the global forecast system at NMC. *Wea. and Forecasting*, **6**, 425-435.

_____, and Coauthors, 2002a: NCEP Dynamical seasonal forecast system 2000. *Bull. Amer. Meteor. Soc.,* **83**, 1019-1037.

_____, W. Ebisuzaki, J. Woollen, S.-K. Yang, J. J. Hnilo, M. Fiorino, and G. L. Potter, 2002b: NCEP-DOE AMIP-II reanalysis (R-2). Dynamical seasonal forecast system 2000. *Bull. Amer. Meteor. Soc.,* **83**, 1631-1643.

Lin, J. W.-B., and J. D. Neelin, 2002: Considerations for stochastic parameterization, *J. Atmos. Sci.*, **59**, 959-975.

Lord, S. J., W. C. Chao, and A. Arakawa, 1982: Interaction of a cumulus cloud ensemble with the large-scale environment. Part IV: The Discrete Model. *J. Atmos. Sci.,* **39**, 104–113.

Pan, H.-L., and W.-S. Wu, 1995: Implementing a mass flux convective parameterization package for the NMC medium-range forecast model. NMC office note 409, 40 pp. [Available from NCEP/EMC, 5200 Auth Road, Camp Springs MD 20746].

Reynolds, R. W., and T. M. Smith, 1994: Improved global sea surface temperature analyses using optimum interpolation. *J. Climate*, **7**, 929-948.

Sela, J., 1980: Spectral modeling at the National Meteorological Center. *Mon. Wea. Rev.*, **108**, 1279-1292.

Wu, X., and M. Yannai, 1994: Effects of vertical wind shear on the cumulus transport of momentum: Observations and parameterization. *J. Atmos. Sci.*, **51**, 1640-1660.

Xie, P., and P. A. Arkin, 1997: Global precipitation: A 17-year monthly analysis based on gauge observations, satellite estimates, and numerical model prediction. *Bull. Amer. Meteor. Soc.,* **78**, 2539-2558.